Available online at www.sciencedirect.com
SCIENCE DIRECT®
Computers and Structures 84 (2006) 1494–1505
Computers & Structures
www.elsevier.com/locate/compstruc

A unified formulation for finite element analysis of piezoelectric adaptive plates

A. Robaldo [a], E. Carrera [a,*], A. Benjeddou [b]

[a] Department of Aerospace Engineering, Politecnico di Torino, Corso Duca degli Abruzzi 24, 10129 Turin, Italy
[b] Institut Supérieur de Mécanique de Paris, LISSMA-Structures, 3 rue Fernand Hainault, 93407 Saint Ouen Cedex, France

Received 24 November 2005; accepted 6 January 2006
Available online 30 May 2006

Abstract

This paper presents some finite elements for the dynamic analysis of laminated plates embedding piezoelectric layers based on the principle of virtual displacements (PVD) and an unified formulation. The description of the unknowns allows to keep the order of the expansion of the variables along the thickness direction as a parameter of the model and at the same time to perform both *equivalent single layer* (ESL) and *layer-wise* (LW) descriptions of the state mechanical variables. The full coupling between the electric and mechanical fields is considered; thus, the electric potential is taken as a state variable of the problem and is assumed LW with an order of the expansion that goes from 1 to 4 as the displacement field. In case of a ESL model the ZZ-function of Murakami has been introduced to recover the *zig-zag* form of the displacement field. Combining all the possible parameters, up to 12 different finite elements are addressed. Numerical results have been given for the free-vibrations frequencies of simply supported plates embedding piezoelectric layers. The lamination of the pure elastic layers has been limited to cross-ply in order to compare numerical results to analytical ones obtained by a Navier-type solution based on the same formulation.

Keywords: Piezoelectric plates; Multilayered plates; Finite elements; Unified formulation; Higher order theories; Free-vibration frequencies

1. Introduction

Due to their potential applications, during the last decades, significant efforts have been devoted to the research on the so-called *smart* structures. Such structures differ from the conventional ones by the presence of elements able to perform as actuators and/or sensors, allowing the structure itself to adapt and/or sense to the external environment. This capability leads to a wide range of applications, in particular in the aerospace field such as vibration suppression, shape adaption of aerodynamic surfaces, noise reduction, precision positioning of antennas, aeroelastic control of lifting surfaces and shape control of optical devices. Even if a variety of different materials can be utilized in smart structures, only piezoelectric ones have shown the capability to perform effectively both as actuators and sensors. Another advantage of piezoelectric materials which explain their widespread use in structural engineering applications is the simple integration with composite structures. Composite structures integrating piezoelectric materials offer the possibility to combine the low density, superior mechanical and thermal properties of composite materials along with sensing, actuation and control. In so doing, many aerospace applications of piezomaterials are concerned with composite structures which are intrinsically multilayered made. Due to the discontinuity of the mechanical and electrical properties at the layer interfaces, multilayered structures embedding piezoelectric layers require accurate electromechanical modeling. In order to anticipate the behavior of smart structures embedding piezoelectric materials and prevent failure mechanisms, an accurate description of the mechanical and electrical fields in the layers is essential, see [1–3].

* Corresponding author. Tel.: +39 011 5646836; fax: +39 011 5646899.
E-mail address: erasmo.carrera@polito.it (E. Carrera).

0045-7949/$ - see front matter
doi:10.1016/j.compstruc.2006.01.029

Multilayered structures exhibit higher transverse shear and transverse normal flexibilities with respect to in-plane deformability along with a discontinuity of the mechanical and electrical properties in the thickness direction. These peculiarities require the displacement field and the transverse stresses to satisfy some conditions which have been summarized by Carrera [4,5] with the acronym C_z^0. In particular the displacement field $\boldsymbol{u}$ should be able to describe sudden changes of slope in correspondence of layer interfaces. This is known as the *zig-zag* effect (ZZ). Although in-plane stresses $\boldsymbol{\sigma}_p$ can be discontinuous, the *Cauchy* theorem demands the continuity of the transverse stresses $\boldsymbol{\sigma}_n$ and the electric transverse displacement D_z and potential Φ through the thickness. This is indicated as *interlaminar continuity* (IC).

For these reasons, the use of plate theories based on the extension of the Kirchhoff hypotheses (classical lamination theory, CLT) and Reissner–Mindlin (first order shear deformation theory, FSDT) for the static and dynamic analysis of piezoelectric plates can lead to inaccurate results. Assessments and reviews on the modeling and analysis of multilayered piezoelectric plates can be found in papers [6,7].

The interest of this paper has been turned towards the calculation of free-vibrations frequencies of multilayered plates embedding piezoelectric layers.

Three-dimensional coupled [8] solution for the free-vibrations analysis of simply supported piezoelectric plates has been proposed in the literature. Several two-dimensional analytical solutions have been also presented, among the others the one by Mitchell and Reddy [9] in which a third-order shear deformation theory (TSDT) has been associated with a layer-wise quadratic electric potential approximation can be remembered. Even if three-dimensional and two-dimensional analytical models have reached an impressive accuracy, the solution of practical problems often demand the use of computational methods such as the finite element method. In literature solid, shell, plate and beam finite elements for the analysis of piezoelectric plates can be found. Interested readers are addressed to the survey on finite element modeling of adaptive structures by Benjeddou [1].

The present paper presents some finite elements for the analysis of multilayered composite plates embedding piezoelectric layers based on the principle of virtual displacements (PVD) and the unified formulation introduced by Carrera [4]. This formulation has already shown all its potentiality as a base for finite elements in the mechanical [10,11] and thermoelastic analysis [12] of multilayered plates. One of the most interesting features of the unified formulation consists in the possibility to keep the order of the expansion of the state variables along the thickness of the plate as a parameter of the model. In so doing, both *equivalent single layer* (ESL) and *layer-wise* (LW) descriptions of the variables are allowed. The displacement unknowns are expanded up to the fourth order through a set of functions F_τ that depend only on the thickness coordinate z. These functions can be simple Taylor polynomials or a manipulation of the Legendre ones respectively for an ESL or a LW description of the laminate. In case of a ESL model the *zig-zag* form has been recovered introducing the ZZ-function of Murakami [13]. The electrical potential assumption has been limited to a LW description and the order of the expansion goes from 1 to 4 as the displacement field. This feature is particularly suitable since electric degrees of freedom (dofs) are often avoided for plates elements [14] or a simple through-thickness linear variation [15,16,17,18] is assumed for the electric potential. One of the few plate elements that consider a quadratic assumption for the electric potential is the work by Carrera [19]. The linear through-thickness hypothesis for the electric potential, as demonstrated by Benjeddou [1], neglects systematically the contribution of the induced potential leading to a partial electromechanical coupling. With the present formulation, the errors induced by the linear assumption of the electric potential can be easily pointed out. In fact, combining all the possible parameters, up to 12 theories are addressed in this work.

Since all the finite elements proposed in this work are based on the PVD, the C_z^0 requirements are not completely satisfied. In particular, the IC condition on the transverse stresses is fulfilled with a post-processing procedure and that of the transverse electric displacement is not considered.

Finite elements based on Reissner mixed variational principle for the analysis of piezolaminated plate structures have been proposed in [20]. In that work, transverse stresses as well as transverse electrical displacement have been taken as additional primary variables fulfilling the interlaminar conditions.

2. Geometry and material assumptions

A multilayered plate is a laminate obtained by stacking rectangular layers until the desired thickness and stiffness are reached. Generally each layer can be made of any kind of material (piezoelectric or purely elastic). Laminae are considered homogeneous, perfectly bonded with each other and operating in the linear elastic range.

To analyze such a typology of structures, a Cartesian coordinate system x, y, z referred to the middle surface is used and it can be seen in Fig. 1 for a plate whose dimensions and thickness are a, b and h. This system is called laminate coordinate system. For the analysis of composite materials, a second coordinate system is needed: the material coordinate system. This is given for each lamina and is commonly indicated by the axes 1, 2, 3. The material coordinate 1-axis is taken to be parallel to the fiber direction, the 2-axis is transverse to the fiber direction in the plane of the lamina while the 3-axis is perpendicular to the lamina. All the material data such as Young moduli and piezoelectric coefficients, are given in the material reference system instead, the analysis of the structure is made in the laminate coordinate system. This implies that the

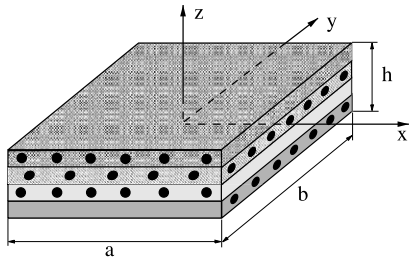

Fig. 1. Geometry and notation for multilayered plates.

constitutive equations are to be written first in the material coordinate system and then in the laminate one. To establish a uniform modeling, all the layers are assumed to be piezoelectric and then for purely elastic ones the piezoelectric coefficients are set to zero. The piezoelectric materials considered in this work are polarized polycrystalline ceramic materials with the crystal symmetry associated to the crystallographic class 2 mm of the hexagonal crystal system (see [21]) polarized along the thickness direction while the composite layers are considered, as usual, orthotropic.

3. Constitutive relations for piezoelectric layers

In the laminate reference system, the constitutive equations for the kth layer take the following form:

$$\boldsymbol{\sigma}^k = \boldsymbol{C}^k \boldsymbol{\varepsilon}_k - \boldsymbol{e}^{k\,\mathrm{T}} \boldsymbol{E}^k \tag{1}$$

$$\boldsymbol{D}^k = \boldsymbol{e}^k \boldsymbol{\varepsilon}^k + \boldsymbol{\epsilon}^k \boldsymbol{E}^k \tag{2}$$

$\boldsymbol{\sigma}^k$ is the stress tensor, $\boldsymbol{C}^k$ is the matrix of the elastic moduli, $\boldsymbol{\varepsilon}^k$ is the linear strain tensor, $\boldsymbol{e}^k$ is the matrix of the piezoelectric constants, $\boldsymbol{E}^k$ is the vector of the electric field, $\boldsymbol{D}^k$ is the vector of the electric displacement, $\boldsymbol{\epsilon}^k$ is the permittivity matrix.

Boldfaced letters are used for arrays, superscript T denotes an operation of transposition.

As one can point out, the coupling between the stresses and the electric field in the kth layer is sustained by the direct (Eq. (2)) and the converse (Eq. (1)) piezoelectric effects.

From now forwards, stresses and strains are going to be separated in in-plane and normal components denoted respectively by the subscripts p and n; thus, using a single subscript notation the explicit form of the constitutive equations is

$$\boldsymbol{\sigma}_p^k = \begin{bmatrix} \sigma_1 \\ \sigma_2 \\ \sigma_6 \end{bmatrix}^k = \begin{bmatrix} C_{11} & C_{12} & C_{16} \\ C_{12} & C_{22} & C_{26} \\ C_{16} & C_{26} & C_{66} \end{bmatrix}^k \begin{bmatrix} \varepsilon_1 \\ \varepsilon_2 \\ \varepsilon_6 \end{bmatrix}^k + \begin{bmatrix} 0 & 0 & C_{13} \\ 0 & 0 & C_{23} \\ 0 & 0 & C_{36} \end{bmatrix}^k \begin{bmatrix} \varepsilon_5 \\ \varepsilon_4 \\ \varepsilon_3 \end{bmatrix}^k = \boldsymbol{C}_{pp}^k \boldsymbol{\varepsilon}_p^k + \boldsymbol{C}_{pn}^k \boldsymbol{\varepsilon}_n^k \tag{3}$$

$$\boldsymbol{\sigma}_n^k = \begin{bmatrix} \sigma_5 \\ \sigma_4 \\ \sigma_3 \end{bmatrix}^k = \begin{bmatrix} 0 & 0 & 0 \\ 0 & 0 & 0 \\ C_{13} & C_{23} & C_{36} \end{bmatrix}^k \begin{bmatrix} \varepsilon_1 \\ \varepsilon_2 \\ \varepsilon_6 \end{bmatrix}^k + \begin{bmatrix} C_{55} & C_{45} & 0 \\ C_{45} & C_{44} & 0 \\ 0 & 0 & C_{33} \end{bmatrix}^k \begin{bmatrix} \varepsilon_5 \\ \varepsilon_4 \\ \varepsilon_3 \end{bmatrix}^k = \boldsymbol{C}_{pn}^{k\,\mathrm{T}} \boldsymbol{\varepsilon}_p^k + \boldsymbol{C}_{nn}^k \boldsymbol{\varepsilon}_n^k \tag{4}$$

The same separation is made on the piezoelectric stiffness $\boldsymbol{e}$ obtaining

$$\boldsymbol{e}_p^k = \begin{bmatrix} 0 & 0 & 0 \\ 0 & 0 & 0 \\ e_{31} & e_{32} & e_{36} \end{bmatrix}^k \quad \text{and} \quad \boldsymbol{e}_n^k = \begin{bmatrix} e_{15} & e_{14} & 0 \\ e_{25} & e_{24} & 0 \\ 0 & 0 & e_{33} \end{bmatrix}^k \tag{5}$$

So, using Eqs. (3)–(5), the constitutive Eqs. (1) and (2) can be written as

$$\boldsymbol{\sigma}_p^k = \boldsymbol{C}_{pp}^k \boldsymbol{\varepsilon}_p^k + \boldsymbol{C}_{pn}^k \boldsymbol{\varepsilon}_n^k - \boldsymbol{C}_p^{k\mathrm{T}} \boldsymbol{E}^k \tag{6}$$

$$\boldsymbol{\sigma}_n^k = \boldsymbol{C}_{pn}^{k\,\mathrm{T}} \boldsymbol{\varepsilon}_p^k + \boldsymbol{C}_{nn}^k \boldsymbol{\varepsilon}_n^k - \boldsymbol{e}_n^{k\mathrm{T}} \boldsymbol{E}^k \tag{7}$$

$$\boldsymbol{D}^k = \boldsymbol{e}_p^k \boldsymbol{\varepsilon}_p^k + \boldsymbol{e}_n^k \boldsymbol{\varepsilon}_n^k + \boldsymbol{\epsilon}^k \boldsymbol{E}^k \tag{8}$$

4. Geometric relations

The strains $\boldsymbol{\varepsilon}_p^k$ and $\boldsymbol{\varepsilon}_n^k$ can be related to the displacement field $\boldsymbol{u}^k$ via geometric relations:

$$\boldsymbol{\epsilon}_{p\mathrm{G}}^k = \boldsymbol{D}_p \boldsymbol{u}^k \tag{9}$$

$$\boldsymbol{\epsilon}_{n\mathrm{G}}^k = (\boldsymbol{D}_{np} + \boldsymbol{D}_{nz}) \boldsymbol{u}^k \tag{10}$$

wherein the differential operator arrays are defined as follows:

$$\boldsymbol{D}_p = \begin{bmatrix} \partial_x & 0 & 0 \\ 0 & \partial_y & 0 \\ \partial_y & \partial_x & 0 \end{bmatrix} \quad \boldsymbol{D}_{np} = \begin{bmatrix} 0 & 0 & \partial_x \\ 0 & 0 & \partial_y \\ 0 & 0 & 0 \end{bmatrix} \quad \boldsymbol{D}_{nz} = \begin{bmatrix} \partial_z & 0 & 0 \\ 0 & \partial_z & 0 \\ 0 & 0 & \partial_z \end{bmatrix} \tag{11}$$

A similar behavior can be observed for the electric field that is related to the electric potential Φ. The electric field $\boldsymbol{E}$ is defined as the gradient of the electric potential Φ:

$$\boldsymbol{E}^k = \begin{bmatrix} -\partial_x \\ -\partial_y \\ -\partial_z \end{bmatrix} \Phi^k = (\boldsymbol{D}_{ep} + \boldsymbol{D}_{ez}) \Phi^k \tag{12}$$

where

$$\boldsymbol{D}_{ep} = \begin{bmatrix} -\partial_x \\ -\partial_y \\ 0 \end{bmatrix} \quad \boldsymbol{D}_{ez} = \begin{bmatrix} 0 \\ 0 \\ -\partial_z \end{bmatrix} \tag{13}$$

All these relations will be used with the *principle of virtual displacements* statement in order to obtain the *stiffness* matrices for the FE model.

5. Unified formulation for displacements and electric potential

Since the proposed formulation is based on the classical PVD, the unknowns of the problem are the displacement field $\boldsymbol{u}^k$ and the electric potential Φ^k. In the framework of the unified formulation introduced in [4], the unknowns are assumed by using a generalized expansion that permits

one to develop both equivalent single layer and layer-wise analyses.

5.1. Equivalent single layer displacements formulation

If an *equivalent single layer* theory is addressed, the unified formulation assumes a displacement field in the form

$$\begin{aligned}\boldsymbol{u}(x,y,z) &= F_b(z)\boldsymbol{u}_b(x,y) + F_r(z)\boldsymbol{u}_r(x,y) + F_t(z)\boldsymbol{u}_t(x,y)\\ &= F_\tau \boldsymbol{u}_\tau \quad \tau = t,r,b\end{aligned} \tag{14}$$

where F_τ are called *thickness functions* and depend only on z. In an *equivalent single layer* theory the thickness functions F_τ are simple Taylor polynomials and then take the form

$$F_b = 1, \quad F_r = z^r, \quad F_t = z^N \quad r = 1,2,\ldots,N-1 \tag{15}$$

where N is the order of the expansion. In this case, the displacement field is independent from the number of layers of the structure. For an ESL theory, the ZZ form of the displacements can be reproduced by referring to Murakami's idea [13] and the displacement model can be written in the following generalized form:

$$\boldsymbol{u} = \boldsymbol{u}_0 + (-1)^k \zeta_k \boldsymbol{u}_\zeta + z^r \boldsymbol{u}_r \quad r = 1,2,\ldots,N; \;\; k = 1,\ldots,N_L \tag{16}$$

where $\zeta_k = \frac{2z_k}{h_k}$ is a non-dimensional layer coordinate (z_k is the physical coordinate of the k-layer whose thickness is h_k) and N_L is the total number of layers.

In generalized form Eq. (16) can be written as Eq. (14), after defining the thickness functions as

$$F_b = 1, \quad F_t = P_z(z) = (-1)^k \zeta_k, \quad F_r = z^r \;\; r = 1,2,\ldots,N \tag{17}$$

5.2. Layer-wise displacements formulation

In a *layer-wise* theory the thickness functions are defined by

$$F_t = \frac{P_0 + P_1}{2}, \quad F_b = \frac{P_0 - P_1}{2}, \quad F_r = P_r - P_{r-2} \quad r = 2,\ldots,N \tag{18}$$

where $P_i = P_i(\zeta_k)$ is the *Legendre* polynomial of ith order defined in the domain $-1 \leqslant \zeta_k \leqslant 1$. The chosen thickness functions have the interesting properties:

$$\zeta_k = \begin{cases} 1: & F_t = 1, \quad F_b = 0, \quad F_r = 0 \\ -1: & F_t = 0, \quad F_b = 1, \quad F_r = 0 \end{cases} \tag{19}$$

Using these definitions, the generalized displacements assumptions of the kth layer can be stated as

$$\begin{aligned}\boldsymbol{u}^k(x,y,z) &= F_b(z)\boldsymbol{u}_b^k(x,y) + F_r(z)\boldsymbol{u}_r^k(x,y) + F_t(z)\boldsymbol{u}_t^k(x,y)\\ &= F_\tau \boldsymbol{u}_\tau^k \quad \text{with } r = 2,\ldots,N; \;\; k = 1,2,\ldots,N_L\end{aligned} \tag{20}$$

Thus, taking into account Eq. (19), the displacement variables $\boldsymbol{u}_b$ and $\boldsymbol{u}_t$ are the actual displacements at the bottom and the top surfaces of the layer and the displacement interlaminar continuity can be easily obtained imposing:

$$\boldsymbol{u}_t^k = \boldsymbol{u}_b^{(k+1)}, \quad \text{with } k = 1,\ldots,N_L - 1 \tag{21}$$

5.3. Electric potential

The electric potential Φ will be written using the same notation of Eq. (20). In this case for the differences of the electric properties of each layer, ESL assumption is not appropriate:

$$\begin{aligned}&\Phi^k = F_t\Phi_t^k + F_b\Phi_b^k + F_r\Phi_r^k = F_\tau\Phi_\tau^k\\ &\text{where } r = 2,\ldots,N; \;\; k = 1,2,\ldots,N_L\end{aligned} \tag{22}$$

The same thickness functions F_τ are used as in the layer-wise displacement case and the interlaminar compatibility conditions of the potential can thus be imposed by

$$\Phi_t^k = \Phi_b^{(k+1)}, \quad k = 1,\ldots,N_L - 1 \tag{23}$$

For convenience, at the moment, the expansion order N of the potential assumption is chosen to be the same as the expansion of the displacement assumption even if theoretically the two orders are totally independent. So, the unified formulation would allow, for example, to perform analyses with a third order expansion for the displacement field and a quadratic assumption for the potential.

5.4. Acronym explanation

The most important aspect of the unified formulation to point out is that using a special assembling procedure, the number of nodes of the element, the order of the expansion and the description of the unknowns can be taken as parameters of the performed analysis. In so doing, different number of nodes per elements and different theories can be tested using the same formulation. In the present work, the number of nodes per element has been limited to 4 and 9 and the order of the expansion can be chosen from 1 to 4. To quickly address the performed analyses, an acronym has been introduced. Fig. 2 explains how the acronym is built. For instance, LD3 is a third order layer-wise theory based on the PVD; ED2 is a parabolic equivalent single layer one; EDZ1 is obtained by adding the Murakami ZZ function to ED1 case.

6. Finite element discretization

The starting point of the finite element formulation using independent variables $\boldsymbol{u}$ and Φ is the *principle of virtual displacement* for piezoelectric media:

$$\int_V (\sigma_{ij}\,\delta\varepsilon_{ij} - D_i\,\delta E_i)\,\mathrm{d}V = \delta L_e - \delta L_{in} = \delta L_e - \int_V \rho\ddot{u}_j\,\delta u_j\,\mathrm{d}V \tag{24}$$

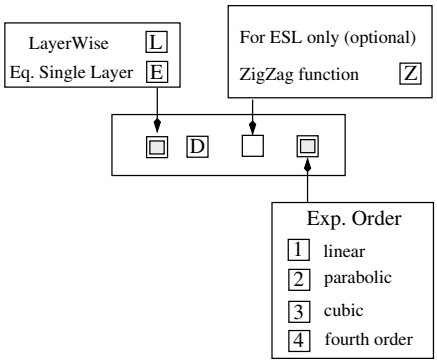

Fig. 2. Explanation of the acronym used in the analysis.

where V is the volume of the plate, t is the time and double dots ($\ddot{}$) indicate twice derivation on time, ρ is the mass density of the layer while δL_e is the variation of the external work, made by external mechanical loads and surface electric charge and δL_{in} is the variation of the work made by inertial loads.

The unknowns are expressed in terms of their nodal values, via the shape functions N_i:

$$\boldsymbol{u}^k_\tau(x,y) = N_i \boldsymbol{q}^k_{\tau i} \quad i = 1,2,\ldots,N_n \tag{25}$$

$$\Phi^k_\tau(x,y) = N_i g^k_{\tau i} \quad i = 1,2,\ldots,N_n \tag{26}$$

where N_n denotes the number of nodes of the element while:

$$\boldsymbol{q}^k_{\tau i} = \begin{bmatrix} q^k_{u_x \tau i} \\ q^k_{u_y \tau i} \\ q^k_{u_z \tau i} \end{bmatrix} \quad g^k_{\tau i} = \begin{bmatrix} g^k_{\phi \tau i} \end{bmatrix} \tag{27}$$

Substituting Eqs. (25) and (26) respectively in Eqs. (14) and (22), the final expressions of the displacement field and the electric potential can be obtained:

$$\boldsymbol{u}^k(x,y,z) = F_\tau N_i \boldsymbol{q}^k_{\tau i} \tag{28}$$

$$\Phi^k = F_\tau N_i g^k_{\tau i} \tag{29}$$

For the whole laminate of N_l layers, from the variational statement in Eq. (24) the following variational equation can be deduced

$$\sum_{k=1}^{N_l} \int_{A_k} \int_{h_k} \left\{ \delta \boldsymbol{\varepsilon}^{k\,\mathrm{T}}_{p\mathrm{G}} \boldsymbol{\sigma}^k_{p\mathrm{C}} + \delta \boldsymbol{\varepsilon}^{k\,\mathrm{T}}_{n\mathrm{G}} \boldsymbol{\sigma}^k_{n\mathrm{C}} - \delta \boldsymbol{E}^{k\,\mathrm{T}}_{\mathrm{G}} \boldsymbol{D}^k_{\mathrm{C}} \right\} \mathrm{d}A_k \, \mathrm{d}z = \delta L_e - \delta L_{in} \tag{30}$$

where A_k is the reference plane of the layer while h_k is its thickness. The subscript C indicates entities evaluated through the constitutive laws (6)–(8) and the subscript G entities evaluated through geometrical relations Eqs. (9), (10) and (12). The unified formulation gives us the possibility of building all the finite element matrices involved in the analysis of multilayered plates from smaller arrays that are called the fundamental nuclei. These arrays have, in the most general case, $[3 \times 3]$ dimension and are therefore assembled in the opportune way depending on the used variable description. The first step in order to obtain the matrices involved in the finite element analysis consists in the substitution of the constitutive Eqs. (6)–(8) into Eq. (30) for the k-layer states. Then

$$\begin{aligned} &\int_{A_k} \int_{h_k} \left\{ \delta \boldsymbol{\varepsilon}^{k\,\mathrm{T}}_{p\mathrm{G}} \left(\boldsymbol{C}^k_{pp} \boldsymbol{\varepsilon}^k_{p\mathrm{G}} + \boldsymbol{C}^k_{pn} \boldsymbol{\varepsilon}^k_{n\mathrm{G}} - \boldsymbol{e}^{k\,\mathrm{T}}_p \boldsymbol{E}^k_G \right) \right. \\ &+ \delta \boldsymbol{\varepsilon}^{k\,\mathrm{T}}_{n\mathrm{G}} \left(\boldsymbol{C}^{k\,\mathrm{T}}_{pn} \boldsymbol{\varepsilon}^k_{p\mathrm{G}} + \boldsymbol{C}^k_{nn} \boldsymbol{\varepsilon}^k_{n\mathrm{G}} - \boldsymbol{e}^{k\,\mathrm{T}}_n \boldsymbol{E}^k_G \right) \\ &\left. - \delta \boldsymbol{E}^{k\,\mathrm{T}}_{\mathrm{G}} \left(\boldsymbol{e}^k_p \boldsymbol{\varepsilon}^k_{p\mathrm{G}} + \boldsymbol{e}^k_n \boldsymbol{\varepsilon}^k_{n\mathrm{G}} + \boldsymbol{\epsilon}^k \boldsymbol{E}^k_G \right) \right\} \mathrm{d}A_k \, \mathrm{d}z = \delta L^k_e - \delta L^k_{in} \end{aligned} \tag{31}$$

introducing the geometric relations (9), (10) and (12), the following statement of the PVD can be obtained for the kth layer:

$$\begin{aligned} &\int_{A_k} \int_{h_k} \left\{ (\boldsymbol{D}_p \delta \boldsymbol{u}^k)^{\mathrm{T}} [(\boldsymbol{C}^k_{pp} \boldsymbol{D}_p + \boldsymbol{C}^k_{pn} (\boldsymbol{D}_{np} + \boldsymbol{D}_{nz})) \boldsymbol{u}^k \right. \\ &- \boldsymbol{e}^{k\,\mathrm{T}}_p (\boldsymbol{D}_{ep} + \boldsymbol{D}_{ez}) \Phi^k] + ((\boldsymbol{D}_{np} + \boldsymbol{D}_{nz}) \delta \boldsymbol{u}^k)^{\mathrm{T}} \\ &\times [(\boldsymbol{C}^{k\,\mathrm{T}}_{pn} \boldsymbol{D}_p + \boldsymbol{C}^k_{nn} (\boldsymbol{D}_{np} + \boldsymbol{D}_{nz})) \boldsymbol{u}^k - \boldsymbol{e}^{k\,\mathrm{T}}_n (\boldsymbol{D}_{ep} + \boldsymbol{D}_{ez}) \Phi^k] \\ &- ((\boldsymbol{D}_{ep} + \boldsymbol{D}_{ez}) \delta \Phi^k)^{\mathrm{T}} [(\boldsymbol{e}^k_p \boldsymbol{D}_p + \boldsymbol{e}^k_n (\boldsymbol{D}_{np} + \boldsymbol{D}_{nz})) \boldsymbol{u}^k \\ &\left. + \boldsymbol{\epsilon}^k (\boldsymbol{D}_{ep} + \boldsymbol{D}_{ez}) \Phi^k] \right\} \mathrm{d}A_k \, \mathrm{d}z = \delta L^k_e - \delta L^k_{in} \end{aligned} \tag{32}$$

Introducing the thickness functions via Eqs. (20) and (22):

$$\begin{aligned} &\int_{A_k} \int_{h_k} \left\{ (\boldsymbol{D}_p F^u_\tau \delta \boldsymbol{u}^k_\tau)^{\mathrm{T}} [(\boldsymbol{C}^k_{pp} \boldsymbol{D}_p + \boldsymbol{C}^k_{pn} (\boldsymbol{D}_{np} + \boldsymbol{D}_{nz})) (F^u_s \boldsymbol{u}^k_s) \right. \\ &- \boldsymbol{e}^{k\,\mathrm{T}}_p (\boldsymbol{D}_{ep} + \boldsymbol{D}_{ez}) (F^e_s \Phi^k_s)] + ((\boldsymbol{D}_{np} + \boldsymbol{D}_{nz}) (F^u_\tau \delta \boldsymbol{u}^k_\tau))^{\mathrm{T}} \\ &\times [(\boldsymbol{C}^{k\,\mathrm{T}}_{pn} \boldsymbol{D}_p + \boldsymbol{C}^k_{nn} (\boldsymbol{D}_{np} + \boldsymbol{D}_{nz})) (F^u_s \boldsymbol{u}^k_s) \\ &- \boldsymbol{e}^{k\,\mathrm{T}}_n (\boldsymbol{D}_{ep} + \boldsymbol{D}_{ez}) (F^e_s \Phi^k_s)] - ((\boldsymbol{D}_{ep} + \boldsymbol{D}_{ez}) (F^e_\tau \delta \Phi^k_\tau))^{\mathrm{T}} \\ &\times [(\boldsymbol{e}^k_p \boldsymbol{D}_p + \boldsymbol{e}^k_n (\boldsymbol{D}_{np} + \boldsymbol{D}_{nz})) (F^u_s \boldsymbol{u}^k_s) \\ &\left. + \boldsymbol{\epsilon}^k (\boldsymbol{D}_{ep} + \boldsymbol{D}_{ez}) (F^e_s \Phi^k_s)] \right\} \mathrm{d}A_k \, \mathrm{d}z = \delta L^k_e - \delta L^k_{in} \end{aligned} \tag{33}$$

where the superscripts u, e on the thickness functions have been introduced to keep memory of their origin.

At last, introducing the shape functions via the substitution of Eqs. (25) and (26) in the previous equation, the following statement of the PVD can be obtained:

$$\begin{aligned} &\int_{A_k} \int_{h_k} \left\{ ((\boldsymbol{D}_p) (F^u_\tau N_i \delta \boldsymbol{q}^k_{\tau i}))^{\mathrm{T}} [(\boldsymbol{C}^k_{pp} \boldsymbol{D}_p + \boldsymbol{C}^k_{pn} (\boldsymbol{D}_{np} + \boldsymbol{D}_{nz})) \right. \\ &\times (F^u_s N_j \boldsymbol{q}^k_{sj}) - \boldsymbol{e}^{k\,\mathrm{T}}_p (\boldsymbol{D}_{ep} + \boldsymbol{D}_{ez}) (F^e_s N_j g^k_{sj})] + ((\boldsymbol{D}_{np} + \boldsymbol{D}_{nz}) \\ &\times (F^u_\tau N_i \delta \boldsymbol{q}^k_{\tau i}))^{\mathrm{T}} [(\boldsymbol{C}^{k\,\mathrm{T}}_{pn} \boldsymbol{D}_p + \boldsymbol{C}^k_{nn} (\boldsymbol{D}_{np} + \boldsymbol{D}_{nz})) (F^u_s N_j \boldsymbol{q}^k_{sj}) \\ &- \boldsymbol{e}^{k\,\mathrm{T}}_n (\boldsymbol{D}_{ep} + \boldsymbol{D}_{ez}) (F^e_s N_j g^k_{sj})] - ((\boldsymbol{D}_{ep} + \boldsymbol{D}_{ez}) (F^e_\tau N_i \delta g^k_{\tau i}))^{\mathrm{T}} \\ &\times [(\boldsymbol{e}^k_p \boldsymbol{D}_p + \boldsymbol{e}^k_n (\boldsymbol{D}_{np} + \boldsymbol{D}_{nz})) (F^u_s N_j \boldsymbol{q}^k_{sj}) \\ &\left. + \boldsymbol{\epsilon}^k (\boldsymbol{D}_{ep} + \boldsymbol{D}_{ez}) (F^e_s N_j g^k_{sj})] \right\} \mathrm{d}A_k \, \mathrm{d}z = \delta L^k_e - \delta L^k_{in} \end{aligned} \tag{34}$$

6.1. Fundamental nuclei

The procedure for obtaining the fundamental nuclei starts separating each term of Eq. (34) and making the following assumptions:

$$\boldsymbol{I}=\begin{bmatrix}1&0&0\\0&1&0\\0&0&1\end{bmatrix}\quad \boldsymbol{I}^{*}=\begin{bmatrix}0\\0\\-1\end{bmatrix} \tag{35}$$

so that we obtain

$$\begin{aligned}
&\delta\boldsymbol{q}^{k\,\mathrm{T}}_{\tau i}\int_{A_k}(\boldsymbol{D}_p^{\mathrm{T}}N_i)\boldsymbol{C}^k_{pp}\left[\int_{h_k}F^u_\tau F^u_s\,\mathrm{d}z\right](\boldsymbol{D}_pN_j)\,\mathrm{d}A_k\boldsymbol{q}^k_{sj}\\
&\quad+\delta\boldsymbol{q}^{k\,\mathrm{T}}_{\tau i}\int_{A_k}(\boldsymbol{D}_p^{\mathrm{T}}N_i)\boldsymbol{C}^k_{pn}\left[\int_{h_k}F^u_\tau F^u_s\,\mathrm{d}z\right](\boldsymbol{D}_{np}N_j)\,\mathrm{d}A_k\boldsymbol{q}^k_{sj}\\
&\quad+\delta\boldsymbol{q}^{k\,\mathrm{T}}_{\tau i}\int_{A_k}(\boldsymbol{D}_p^{\mathrm{T}}N_i)\boldsymbol{C}^k_{pn}\left[\int_{h_k}F^u_\tau F^u_{s_{,z}}\,\mathrm{d}z\right](N_j\boldsymbol{I})\,\mathrm{d}A_k\boldsymbol{q}^k_{sj}\\
&\quad-\delta\boldsymbol{q}^{k\,\mathrm{T}}_{\tau i}\int_{A_k}(\boldsymbol{D}_p^{\mathrm{T}}N_i)\boldsymbol{e}^{k\mathrm{T}}_p\left[\int_{h_k}F^u_\tau F^e_s\,\mathrm{d}z\right](\boldsymbol{D}_{ep}N_j)\,\mathrm{d}A_kg^k_{sj}\\
&\quad-\delta\boldsymbol{q}^{k\,\mathrm{T}}_{\tau i}\int_{A_k}(\boldsymbol{D}_p^{\mathrm{T}}N_i)\boldsymbol{e}^{k\mathrm{T}}_p\left[\int_{h_k}F^u_\tau F^e_{s_{,z}}\,\mathrm{d}z\right](N_j\boldsymbol{I}^{*})\,\mathrm{d}A_kg^k_{sj}\\
&\quad+\delta\boldsymbol{q}^{k\,\mathrm{T}}_{\tau i}\int_{A_k}(\boldsymbol{D}_{np}^{\mathrm{T}}N_i)\boldsymbol{C}^{k\ \mathrm{T}}_{pn}\left[\int_{h_k}F^u_\tau F^u_s\,\mathrm{d}z\right](\boldsymbol{D}_pN_j)\,\mathrm{d}A_k\boldsymbol{q}^k_{sj}\\
&\quad+\delta\boldsymbol{q}^{k\,\mathrm{T}}_{\tau i}\int_{A_k}(\boldsymbol{D}_{np}^{\mathrm{T}}N_i)\boldsymbol{C}^k_{nn}\left[\int_{h_k}F^u_\tau F^u_s\,\mathrm{d}z\right](\boldsymbol{D}_{np}N_j)\,\mathrm{d}A_k\boldsymbol{q}^k_{sj}\\
&\quad+\delta\boldsymbol{q}^{k\,\mathrm{T}}_{\tau i}\int_{A_k}(\boldsymbol{D}_{np}^{\mathrm{T}}N_i)\boldsymbol{C}^k_{nn}\left[\int_{h_k}F^u_\tau F^u_{s_{,z}}\,\mathrm{d}z\right](N_j\boldsymbol{I})\,\mathrm{d}A_k\boldsymbol{q}^k_{sj}\\
&\quad-\delta\boldsymbol{q}^{k\,\mathrm{T}}_{\tau i}\int_{A_k}(\boldsymbol{D}_{np}^{\mathrm{T}}N_i)\boldsymbol{e}^{k\mathrm{T}}_n\left[\int_{h_k}F^u_\tau F^e_s\,\mathrm{d}z\right](\boldsymbol{D}_{ep}N_j)\,\mathrm{d}A_kg^k_{sj}\\
&\quad-\delta\boldsymbol{q}^{k\,\mathrm{T}}_{\tau i}\int_{A_k}(\boldsymbol{D}_{np}^{\mathrm{T}}N_i)\boldsymbol{e}^{k\mathrm{T}}_n\left[\int_{h_k}F^u_\tau F^e_{s_{,z}}\,\mathrm{d}z\right](N_j\boldsymbol{I}^{*})\,\mathrm{d}A_kg^k_{sj}\\
&\quad+\delta\boldsymbol{q}^{k\,\mathrm{T}}_{\tau i}\int_{A_k}N_i\boldsymbol{C}^{k\ \mathrm{T}}_{pn}\left[\int_{h_k}F^u_{\tau_{,z}}F^u_s\,\mathrm{d}z\right](\boldsymbol{D}_pN_j)\,\mathrm{d}A_k\boldsymbol{q}^k_{sj}\\
&\quad+\delta\boldsymbol{q}^{k\,\mathrm{T}}_{\tau i}\int_{A_k}N_i\boldsymbol{C}^k_{nn}\left[\int_{h_k}F^u_{\tau_{,z}}F^u_s\,\mathrm{d}z\right](\boldsymbol{D}_{np}N_j)\,\mathrm{d}A_k\boldsymbol{q}^k_{sj}\\
&\quad+\delta\boldsymbol{q}^{k\,\mathrm{T}}_{\tau i}\int_{A_k}N_i\boldsymbol{C}^k_{nn}\left[\int_{h_k}F^u_{\tau_{,z}}F^u_{s_{,z}}\,\mathrm{d}z\right](N_j\boldsymbol{I})\,\mathrm{d}A_k\boldsymbol{q}^k_{sj}\\
&\quad-\delta\boldsymbol{q}^{k\,\mathrm{T}}_{\tau i}\int_{A_k}N_i\boldsymbol{e}^{k\mathrm{T}}_n\left[\int_{h_k}F^u_{\tau_{,z}}F^e_s\,\mathrm{d}z\right](\boldsymbol{D}_{ep}N_j)\,\mathrm{d}A_kg^k_{sj}\\
&\quad-\delta\boldsymbol{q}^{k\,\mathrm{T}}_{\tau i}\int_{A_k}N_i\boldsymbol{e}^{k\mathrm{T}}_n\left[\int_{h_k}F^u_{\tau_{,z}}F^e_{s_{,z}}\,\mathrm{d}z\right](N_j\boldsymbol{I}^{*})\,\mathrm{d}A_kg^k_{sj}\\
&\quad-\delta g^{k\,\mathrm{T}}_{\tau i}\int_{A_k}(\boldsymbol{D}_{ep}^{\mathrm{T}}N_i)\boldsymbol{e}^k_p\left[\int_{h_k}F^e_\tau F^u_s\,\mathrm{d}z\right](\boldsymbol{D}_pN_j)\,\mathrm{d}A_k\boldsymbol{q}^k_{sj}\\
&\quad-\delta g^{k\,\mathrm{T}}_{\tau i}\int_{A_k}(\boldsymbol{D}_{ep}^{\mathrm{T}}N_i)\boldsymbol{e}^k_n\left[\int_{h_k}F^e_\tau F^u_s\,\mathrm{d}z\right](\boldsymbol{D}_{np}N_j)\,\mathrm{d}A_k\boldsymbol{q}^k_{sj}\\
&\quad-\delta g^{k\,\mathrm{T}}_{\tau i}\int_{A_k}(\boldsymbol{D}_{ep}^{\mathrm{T}}N_i)\boldsymbol{e}^k_n\left[\int_{h_k}F^e_\tau F^u_{s_{,z}}\,\mathrm{d}z\right](N_j\boldsymbol{I})\,\mathrm{d}A_k\boldsymbol{q}^k_{sj}\\
&\quad-\delta g^{k\,\mathrm{T}}_{\tau i}\int_{A_k}(\boldsymbol{D}_{ep}^{\mathrm{T}}N_i)\boldsymbol{\epsilon}^k\left[\int_{h_k}F^e_\tau F^e_s\,\mathrm{d}z\right](\boldsymbol{D}_{ep}N_j)\,\mathrm{d}A_kg^k_{sj}\\
&\quad-\delta g^{k\,\mathrm{T}}_{\tau i}\int_{A_k}(\boldsymbol{D}_{ep}^{\mathrm{T}}N_i)\boldsymbol{\epsilon}^k\left[\int_{h_k}F^e_\tau F^e_{s_{,z}}\,\mathrm{d}z\right](N_j\boldsymbol{I}^{*})\,\mathrm{d}A_kg^k_{sj}\\
&\quad-\delta g^{k\,\mathrm{T}}_{\tau i}\int_{A_k}(N_i\boldsymbol{I}^{*})^{\mathrm{T}}\boldsymbol{e}^k_p\left[\int_{h_k}F^e_{\tau_{,z}}F^u_s\,\mathrm{d}z\right](\boldsymbol{D}_pN_j)\,\mathrm{d}A_k\boldsymbol{q}^k_{sj}\\
&\quad-\delta g^{k\,\mathrm{T}}_{\tau i}\int_{A_k}(N_i\boldsymbol{I}^{*})^{\mathrm{T}}\boldsymbol{e}^k_n\left[\int_{h_k}F^e_{\tau_{,z}}F^u_s\,\mathrm{d}z\right](\boldsymbol{D}_{np}N_j)\,\mathrm{d}A_k\boldsymbol{q}^k_{sj}\\
&\quad-\delta g^{k\,\mathrm{T}}_{\tau i}\int_{A_k}(N_i\boldsymbol{I}^{*})^{\mathrm{T}}\boldsymbol{e}^k_n\left[\int_{h_k}F^e_{\tau_{,z}}F^u_{s_{,z}}\,\mathrm{d}z\right](N_j\boldsymbol{I}^{*})\,\mathrm{d}A_k\boldsymbol{q}^k_{sj}\\
&\quad-\delta g^{k\,\mathrm{T}}_{\tau i}\int_{A_k}(N_i\boldsymbol{I}^{*})^{\mathrm{T}}\boldsymbol{\epsilon}^k\left[\int_{h_k}F^e_{\tau_{,z}}F^e_s\,\mathrm{d}z\right](\boldsymbol{D}_{ep}N_j)\,\mathrm{d}A_kg^k_{sj}\\
&\quad-\delta g^{k\,\mathrm{T}}_{\tau i}\int_{A_k}(N_i\boldsymbol{I}^{*})^{\mathrm{T}}\boldsymbol{\epsilon}^k\left[\int_{h_k}F^e_{\tau_{,z}}F^e_{s_{,z}}\,\mathrm{d}z\right](N_j\boldsymbol{I}^{*})\,\mathrm{d}A_kg^k_{sj}\\
&\quad=\delta L^k_e-\delta L^k_{in}
\end{aligned} \tag{36}$$

At this point, it is necessary to develop the term related to dynamics δL_{in}, remembering Eq. (24) it can be written at layer level as

$$\delta L^k_{in}=\int_{A_k}\int_{h_k}\rho^k\delta\boldsymbol{u}^{k\mathrm{T}}\ddot{\boldsymbol{u}}^k\,\mathrm{d}A_k\,\mathrm{d}z \tag{37}$$

introducing in the acceleration term the thickness functions and the shape functions as it has been done for displacements we obtain

$$\ddot{\boldsymbol{u}}^k=F^u_\tau N_i\ddot{\boldsymbol{q}}^k_{\tau i} \tag{38}$$

and substituting Eqs. (28) and (38) in Eq. (37) we get

$$\delta L^k_{in}=\delta\boldsymbol{q}^{k\,\mathrm{T}}_{\tau i}\int_{A_k}\rho^k(N_i\boldsymbol{I})\left[\int_{h_k}F^u_\tau F^u_s\,\mathrm{d}z\right](N_j\boldsymbol{I})\,\mathrm{d}A_k\ddot{\boldsymbol{q}}^k_{sj} \tag{39}$$

Since the present paper is addressed towards the dynamic analysis, the term related to the external load is not considered.

6.2. Finite element matrices and governing equations

Introducing the following notations:

$$(E^{\alpha\beta}_{\tau s},E^{\alpha\beta}_{\tau_{,z}s},E^{\alpha\beta}_{\tau s_{,z}},E^{\alpha\beta}_{\tau_{,z}s_{,z}})=\int_{h_k}(F^\alpha_\tau F^\beta_s,F^\alpha_{\tau_{,z}}F^\beta_s,F^\alpha_\tau F^\beta_{s_{,z}},F^\alpha_{\tau_{,z}}F^\beta_{s_{,z}})\,\mathrm{d}z \tag{40}$$

with α and β that can assume the values: u, e and regrouping opportunely the terms of Eqs. (34) and (39) the following terms can be easily obtained:

$$\begin{aligned}
\boldsymbol{K}^{k\tau sij}_{uu}=\int_{A_k}&[(\boldsymbol{D}_p^{\mathrm{T}}N_i)(\boldsymbol{C}^k_{pp}E^{uu}_{\tau s}(\boldsymbol{D}_pN_j)+\boldsymbol{C}^k_{pn}E^{uu}_{\tau s}(\boldsymbol{D}_{np}N_j)\\
&+\boldsymbol{C}^k_{pn}E^{uu}_{\tau s_{,z}}(N_j\boldsymbol{I}))+(\boldsymbol{D}_{np}^{\mathrm{T}}N_i)(\boldsymbol{C}^{k\ \mathrm{T}}_{pn}E^{uu}_{\tau s}(\boldsymbol{D}_pN_j)\\
&+\boldsymbol{C}^k_{nn}E^{uu}_{\tau s}(\boldsymbol{D}_{np}N_j)+\boldsymbol{C}^k_{nn}E^{uu}_{\tau s_{,z}}(N_j\boldsymbol{I}))\\
&+N_i(\boldsymbol{C}^{k\ \mathrm{T}}_{pn}E^{uu}_{\tau_{,z}s}(\boldsymbol{D}_pN_j)+\boldsymbol{C}^k_{nn}E^{uu}_{\tau_{,z}s}(\boldsymbol{D}_{np}N_j)\\
&+\boldsymbol{C}^k_{nn}E^{uu}_{\tau_{,z}s_{,z}}(N_j\boldsymbol{I}))]\,\mathrm{d}A_k
\end{aligned} \tag{41}$$

$$\begin{aligned}
\boldsymbol{K}^{k\tau sij}_{ue}=-\int_{A_k}&[(\boldsymbol{D}_p^{\mathrm{T}}N_i)\boldsymbol{e}^{k\mathrm{T}}_p(E^{ue}_{\tau s}(\boldsymbol{D}_{ep}N_j)+E^{ue}_{\tau s_{,z}}(N_j\boldsymbol{I}^{*}))\\
&+(\boldsymbol{D}_{np}^{\mathrm{T}}N_i)\boldsymbol{e}^{k\mathrm{T}}_n(E^{ue}_{\tau s}(\boldsymbol{D}_{ep}N_j)+E^{ue}_{\tau s_{,z}}(N_j\boldsymbol{I}^{*}))\\
&+N_i\boldsymbol{e}^{k\mathrm{T}}_n(E^{ue}_{\tau_{,z}s}(\boldsymbol{D}_{ep}N_j)+E^{ue}_{\tau_{,z}s_{,z}}(N_j\boldsymbol{I}^{*}))]\,\mathrm{d}A_k
\end{aligned} \tag{42}$$

$$\boldsymbol{K}_{eu}^{k\tau sij} = -\int_{A_k} [(\boldsymbol{D}_{ep}^{\mathrm{T}} N_i)(\boldsymbol{e}_p^k E_{\tau s}^{eu}(\boldsymbol{D}_p N_j) + \boldsymbol{e}_n^k E_{\tau s}^{eu}(\boldsymbol{D}_{np} N_j) + \boldsymbol{e}_n^k E_{\tau s_{,z}}^{eu}(N_j \boldsymbol{I})) + (N_i \boldsymbol{I}^*)^{\mathrm{T}}(\boldsymbol{e}_p^k E_{\tau_{,z} s}^{eu}(\boldsymbol{D}_p N_j) + \boldsymbol{e}_n^k E_{\tau_{,z} s}^{eu}(\boldsymbol{D}_{np} N_j) + \boldsymbol{e}_n^k E_{\tau_{,z} s_{,z}}^{eu}(N_j \boldsymbol{I}))]\,\mathrm{d}A_k \quad (43)$$

$$\boldsymbol{K}_{ee}^{k\tau sij} = -\int_{A_k} [(\boldsymbol{D}_{ep}^{\mathrm{T}} N_i)\boldsymbol{\epsilon}^k(E_{\tau s}^{ee}(\boldsymbol{D}_{ep} N_j) + E_{\tau s_{,z}}^{ee}(N_j \boldsymbol{I}^*)) + (N_i \boldsymbol{I}^*)^{\mathrm{T}}\boldsymbol{\epsilon}^k(E_{\tau_{,z} s}^{ee}(\boldsymbol{D}_{ep} N_j) + E_{\tau_{,z} s_{,z}}^{ee}(N_j \boldsymbol{I}^*))]\,\mathrm{d}A_k \quad (44)$$

$$\boldsymbol{M}_{u\ddot{u}}^{k\tau sij} = \int_{A_k} \rho^k (N_i \boldsymbol{I}) E_{\tau s}^{uu}(N_j \boldsymbol{I})\,\mathrm{d}A_k \quad (45)$$

that are the fundamental nuclei from which the *stiffness* matrices and the governing equations involved in the finite element analysis can be derived.

The dimensions of the fundamental nuclei are summarized in Table 1: Now considering that virtual variations are independent and arbitrary, two governing equations can be written as

$$\delta \boldsymbol{q}_{\tau i}^{k\,\mathrm{T}} : \boldsymbol{K}_{uu}^{k\tau sij} \boldsymbol{q}_{sj}^k + \boldsymbol{K}_{ue}^{k\tau sij} g_{sj}^k = -\boldsymbol{M}_{u\ddot{u}}^{k\tau sij} \ddot{\boldsymbol{q}}_{sj}^k \quad (46)$$

$$\delta g_{\tau i}^{k\,\mathrm{T}} : \boldsymbol{K}_{eu}^{k\tau sij} \boldsymbol{q}_{sj}^k + \boldsymbol{K}_{ee}^{k\tau sij} g_{sj}^k = 0 \quad (47)$$

Eqs. (46) and (47) are valid just at nodal level of a one layer structure; in order to obtain the governing equations for all the structure, the fundamental nuclei should be opportunely assembled expanding the indices i, j, τ, s up to their extents.

Table 1
Dimensions of the fundamental nuclei

Fundamental nucleus	Dimension
$\boldsymbol{K}_{uu}^{k\tau sij}$	$[3\times 3]$
$\boldsymbol{K}_{ue}^{k\tau sij}$	$[3\times 1]$
$\boldsymbol{K}_{eu}^{k\tau sij}$	$[1\times 3]$
$\boldsymbol{K}_{ee}^{k\tau sij}$	$[1\times 1]$
$\boldsymbol{M}_{u\ddot{u}}^{k\tau sij}$	$[3\times 3]$

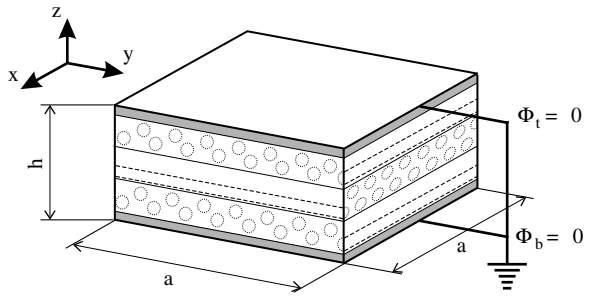

Fig. 3. Schematic representation of the analyzed hybrid sandwich plate. Courtesy by [22].

Table 2
Elastic, piezoelectric and dielectric properties of used materials

Property	PZT-4	G_r/E_p
E_1 (GPa)	81.3	132.38
E_2 (GPa)	81.3	10.756
E_3 (GPa)	64.5	10.756
ν_{12}	0.329	0.24
ν_{13}	0.432	0.24
ν_{23}	0.432	0.49
G_{23} (GPa)	25.6	3.606
G_{13} (GPa)	25.6	5.6537
G_{12} (GPa)	30.6	5.6537
e_{15} (C/m^2)	12.72	0
e_{24} (C/m^2)	12.72	0
e_{31} (C/m^2)	−5.20	0
e_{32} (C/m^2)	−5.20	0
e_{33} (C/m^2)	15.08	0
ϵ_{11}/ϵ_0	1475	3.5
ϵ_{22}/ϵ_0	1475	3.0
ϵ_{33}/ϵ_0	1300	3.0

Table 3
Convergence analysis Q4 ED4 element (ED4 Q4 int. type = SI)

Mesh	$S=4$			$S=50$		
	Mode 1	Mode 2	Mode 3	Mode 1	Mode 2	Mode 3
3D exact [8]	96,929.9	194,255	327,663	746.752	15,540.4	26,828.0
cf. [2]	98,246.6 (+1.35%)	194,255 (+0.00%)	335,395 (+2.36%)	746.837 (−2.34%)	15,540.4 (+0.00%)	26,831.7 (+0.01%)
[2 × 2]	116,896 (+20.6%)	257,321 (+32.4%)	470,630 (+43.6%)	1019.87 (+33.3%)	20,585.7 (+32.4%)	53,066.8 (+97.8%)
[4 × 4]	102,416 (+5.66%)	208,615 (+7.39%)	335,491 (+2.38%)	803.251 (+5.03%)	16,689.9 (+7.39%)	28,567.6 (+6.48%)
[6 × 6]	99,649.1 (+2.80%)	200,510 (+3.22%)	329,325 (+0.50%)	771.082 (+0.82%)	16,040.7 (+3.21%)	27,113.2 (+1.06%)
[10 × 10]	98,240.8 (+1.35%)	196,483 (+1.14%)	328,912 (+0.38%)	755.382 (−1.22%)	15,718.6 (+1.14%)	26,930.6 (+0.38%)
[12 × 12]	97,998.3 (+1.10%)	195,799 (+0.79%)	328,530 (+0.26%)	748.907 (−2.07%)	15,663.9 (+0.79%)	26,899.2 (+0.26%)

First three circular frequencies (ω/100 rad/s) for the single piezoceramic layer plate and relative errors with respect 3D exact solution [8].

Table 4
Convergence analysis Q9 ED4 element (ED4 Q9 int. type = SI)

Mesh	$S=4$			$S=50$		
	1	2	3	1	2	3
3D exact [8]	96,929.9	194,255	327,663	746.752	15,540.4	26,828.0
cf. [2]	98,246.6 (+1.35%)	194,255 (+0.00%)	335,395 (+2.36%)	746.837 (−2.34%)	15,540.4 (+0.00%)	26,831.7 (+0.01%)
[2 × 2]	98,170.9 (+1.28%)	195,903 (+0.84%)	328,397 (+0.22%)	754.532 (−1.33%)	15,670.8 (+0.83%)	26,887.3 (+0.22%)
[4 × 4]	97,508.4 (+0.59%)	194,372 (+0.06%)	327,729 (+0.02%)	747.283 (−2.28%)	15,548.6 (+0.05%)	26,832.5 (+0.01%)
[6 × 6]	97,463.7 (+0.55%)	194,280 (+0.01%)	327,678 (+0.00%)	746.876 (−2.33%)	15,542.0 (+0.01%)	26,828.9 (+0.00%)
[10 × 10]	97,321.4 (+0.40%)	194,264 (+0.00%)	327,670 (+0.00%)	746.834 (−2.34%)	15,542.0 (+0.01%)	26,828.2 (+0.00%)

First three circular frequencies ($\omega/100$ rad/s) for the single piezoceramic layer plate and relative errors with respect 3D exact solution [8].

Since this procedure does not differ from the pure mechanical case, it has not been reported here. Interested readers can find a detailed description of this procedure in [11,12,22].

Once the fundamental nuclei have been assembled at structure level the governing equations take the following form:

$$\boldsymbol{K}_{uu}\boldsymbol{q} + \boldsymbol{K}_{ue}\boldsymbol{g} = -\boldsymbol{M}_{uu}\ddot{\boldsymbol{q}} \tag{48}$$

$$\boldsymbol{K}_{eu}\boldsymbol{q} + \boldsymbol{K}_{ee}\boldsymbol{g} = 0 \tag{49}$$

where $\boldsymbol{q}$ and $\boldsymbol{g}$ are the vectors of the unknown degrees of freedom related respectively to the displacement field and the electric potential.

7. Free-vibration problem

Assuming the following expansion of the variables in the time domain:

$$\boldsymbol{q} = \boldsymbol{Q}\mathrm{e}^{\mathrm{i}\omega t} \quad \boldsymbol{g} = \boldsymbol{G}\mathrm{e}^{\mathrm{i}\omega t} \tag{50}$$

the governing Eqs. (48) and (49) can be rewritten in the following form:

$$\left(\begin{bmatrix}\boldsymbol{K}_{uu} & \boldsymbol{K}_{ue}\\ \boldsymbol{K}_{eu} & \boldsymbol{K}_{ee}\end{bmatrix} - \omega^2\begin{bmatrix}\boldsymbol{M}_{uu} & 0\\ 0 & 0\end{bmatrix}\right)\begin{bmatrix}\boldsymbol{Q}\\ \boldsymbol{G}\end{bmatrix} = \boldsymbol{0} \tag{51}$$

Many degrees of freedom are *massless*. The zero-mass degrees of freedom are here eliminated by *static condensation*. This procedure requires to solve the second equation of the system in Eq. (51) for $\boldsymbol{g}$:

$$\boldsymbol{g} = -\boldsymbol{K}_{ee}^{-1}\boldsymbol{K}_{eu}\boldsymbol{Q} \tag{52}$$

and then substitute it in the first equation of the same system, leading to

$$(\boldsymbol{K}_{uu}^{*} - \omega^2\boldsymbol{M}_{uu})\boldsymbol{Q} = \boldsymbol{0} \tag{53}$$

where

$$\boldsymbol{K}_{uu}^{*} = \boldsymbol{K}_{uu} - \boldsymbol{K}_{ue}\boldsymbol{K}_{ee}^{-1}\boldsymbol{K}_{eu} \tag{54}$$

In order to obtain the classical form of an eigenvalue problem, Eq. (54) has been pre-multiply by the inverse of the mass matrix obtaining

$$(\boldsymbol{A} - \omega^2\boldsymbol{I}_d)\boldsymbol{Q} = \boldsymbol{0} \tag{55}$$

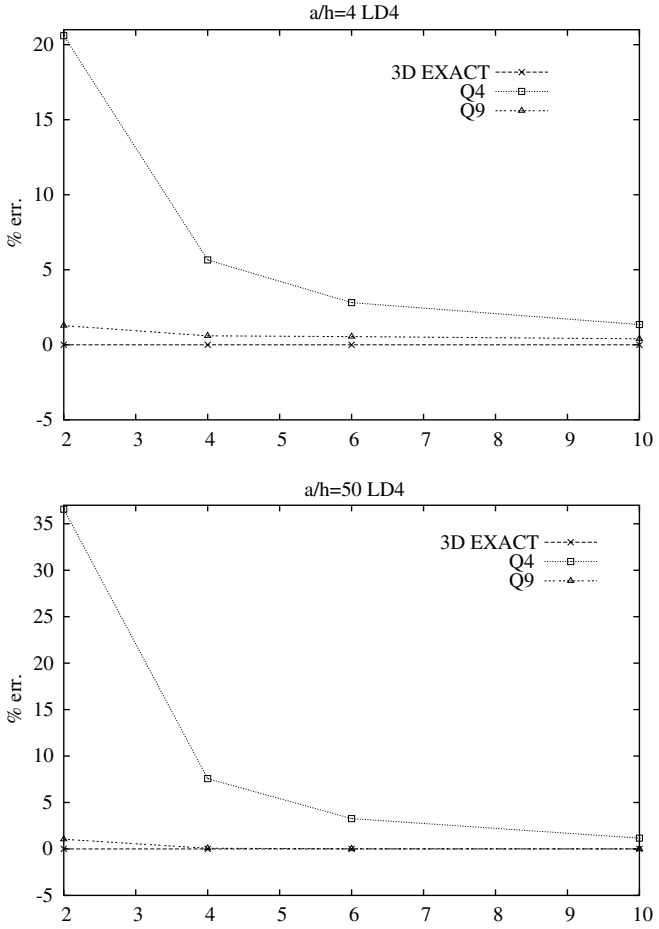

Fig. 4. Convergence analysis of the fundamental frequency for the single piezoceramic layer plate.

where

$$\boldsymbol{A} = \boldsymbol{M}_{uu}^{-1}\boldsymbol{K}_{uu} \tag{56}$$

and $\boldsymbol{I}_d$ is the identity matrix. Eq. (55) is first solved to obtain eigenfrequencies and corresponding eigenvectors (nodal displacements), then the electric potential is computed a posteriori using Eq. (52).

8. Numerical validation and results

In the attempt to verify the present formulation, numerical results for simply supported square plates have been addressed. The two cases considered in the present paper have been among those for which exact analytical solution is present in literature. The reference paper for the two cases taken into consideration is the work by Heyliger and Saravanos [8].

In order to check the implementation of piezoelectric layers into the finite element based on the unified formulation, the first case is about a square plate of side length a and total thickness h made by a single piezoelectric layer. The plate is simply supported and short circuited $\Phi = 0$.

The second case is a more realistic hybrid piezoelectric-elastic sandwich plate that consists of a symmetric three-layer cross-ply (0/90/0) graphite/epoxy laminate core and two $0.1h$-thick piezoceramic faces (see Fig. 3). As for the first case, the electric boundary conditions are those of a short circuited plate.

The properties of the considered materials are listed in Table 2.

Since both thin and thick plates have been analyzed, according to what done in [11] the reduced selective integration (SI) has been implemented in addition to the normal one (NI) in order to mitigate the possible presence of the *shear locking* phenomenon.

8.1. Single piezoceramic layer plate

For this case, a convergence analysis for two side-to-thickness ratios ($S = a/h$) and for both four (Q4) and nine (Q9) node elements have been conducted and results are listed in Tables 3 and 4 and also visible in Fig. 4. A LW formulation with a four order expansion (LD4) has been used for the convergence analysis even if not necessary since this is a single layer plate. The Q9 element presents a good convergence to the exact solution also with a mesh of $[4 \times 4]$. The relative errors with respect to the exact solution for the first three frequencies in this case are respectively:

Table 5
First three thickness circular frequencies ($\omega/100$ rad/s) for the hybrid sandwich plate (LW elements) (Q9 mesh $[4 \times 4]$)

Mesh		$S = 4$			$S = 50$		
		1	2	3	1	2	3
3D exact [8]		57,074.5	191,301	250,769	618.118	15,681.6	21,492.8
cf. [2]		58,216.1 (+2.00%)	196,018 (+2.46%)	268,650 (+7.13%)	618.435 (+0.05%)	15,684.0 (+0.01%)	21,499.4 (+0.03%)
LD4	SI	57,096.9 (+0.03%)	191,361 (+0.03%)	250,803 (+0.01%)	618.450 (+0.05%)	15,686.9 (+0.03%)	21,560.4 (+0.31%)
	NI	57,116.9 (+0.07%)	191,364 (+0.03%)	250,815 (+0.01%)	624.635 (+1.05%)	16,686.9 (+6.41%)	21,497.3 (+0.02%)
	CF	57,074.0 (+0.00%)	191,301 (+0.00%)	250,768 (+0.00%)	618.104 (+0.00%)	15,681.6 (+0.00%)	21,492.6 (+0.00%)
LD3	SI	57,097.2 (+0.04%)	191,361 (+0.03%)	250,803 (+0.01%)	618.450 (+0.05%)	15,686.9 (+0.03%)	21,560.4 (+0.31%)
	NI	57,117.6 (+0.07%)	191,369 (+0.03%)	250,821 (+0.02%)	624.640 (+1.05%)	15,686.9 (+0.03%)	21,497.3 (+0.02%)
	CF	57,074.0 (+0.00%)	191,301 (+0.00%)	250,768 (+0.00%)	618.104 (+0.00%)	15,681.6 (+0.00%)	21,492.6 (+0.00%)
LD2	SI	57,105.1 (+0.05%)	191,371 (+0.03%)	250,821 (−0.19%)	618.450 (+0.05%)	15,686.9 (+0.03%)	21,562.4 (+0.32%)
	NI	57,125.6 (+0.07%)	191,379 (+0.04%)	250,838 (+0.02%)	624.642 (+1.05%)	15,686.9 (+0.03%)	21,497.3 (+0.02%)
	CF	57,081.9 (+0.01%)	191,311 (+0.00%)	250,786 (+0.00%)	618.105 (+0.00%)	15,681.6 (+0.00%)	21,492.6 (+0.00%)
LD1	SI	57,275.5 (+0.35%)	194,907 (+1.88%)	255,689 (+1.96%)	619.473 (+0.21%)	15,688.8 (+0.04%)	21,499.2 (+0.03%)
	NI	57,296.9 (+0.07%)	194,908 (+1.88%)	255,698 (+1.96%)	625.584 (+1.20%)	15,688.8 (+0.04%)	21,499.2 (+0.03%)
	CF	57,252.5 (+0.31%)	194,840 (+1.85%)	255,646 (+1.94%)	619.022 (+0.14%)	15,683.4 (+0.01%)	21,499.4 (+0.03%)

SI and NI indicate respectively selected, and normal integration. CF refers to closed form solution [22].

Table 6
First three thickness circular frequencies (ω/100 rad/s) for the hybrid sandwich plate (EDZ elements) (Q9 mesh [4 × 4])

Mesh		$S = 4$			$S = 50$		
		1	2	3	1	2	3
3D exact [8]		57,074.5	191,301	250,769	618.118	15,681.6	21,492.8
cf. [2]		58,216.1 (+2.00%)	196,018 (+2.46%)	268,650 (+7.13%)	618.435 (+0.05%)	15,684.0 (+0.01%)	21,499.4 (+0.03%)
EDZ3	SI	57,681.4 (+1.06%)	195,779 (+2.34%)	259,632 (+3.53%)	618.831 (+0.11%)	15,692.4 (+0.06%)	21,501.2 (+0.03%)
	NI	57,702.7 (+1.01%)	195,779 (+2.34%)	259,637 (+3.53%)	624.994 (+1.11%)	15,692.4 (+0.06%)	21,501.2 (+0.03%)
	CF	56,656.1 (−0.73%)	195,711 (+2.33%)	259,022 (+3.29%)	618.382 (+0.04%)	15,687.1 (+0.03%)	21,496.5 (+0.01%)
EDZ2	SI	60,629.7 (+6.22%)	195,790 (+2.34%)	260,923 (+4.04%)	619.496 (+0.22%)	15,698.9 (+0.11%)	21,501.2 (+0.03%)
	NI	60,650.9 (+6.26%)	195,790 (+2.34%)	260,927 (+4.05%)	626.193 (+1.30%)	15,698.9 (+0.11%)	21,501.3 (+0.04%)
	CF	60,605.5 (+6.18%)	195,722 (+2.31%)	260,861 (+4.02%)	619.046 (+0.15%)	15,693.6 (+0.07%)	21,496.5 (+0.01%)
EDZ1	SI	63,229.7 (+10.7%)	196,036 (+2.47%)	266,275 (+6.18%)	688.548 (+11.3%)	15,699.0 (+0.11%)	21,503.2 (+0.04%)
	NI	63,250.9 (+10.8%)	196,036 (+2.47%)	266,275 (+6.18%)	694.604 (+12.3%)	15,699.0 (+0.11%)	21,503.2 (+0.04%)
	CF	63,204.7 (+10.7%)	195,965 (+2.43%)	266,196 (+6.15%)	688.082 (+0.07%)	15,693.6 (+0.07%)	21,496.5 (+0.01%)

SI and NI indicate respectively selected, and normal integration. CF refers to closed form solution [22].

Table 7
First three thickness circular frequencies (ω/100 rad/s) for the hybrid sandwich plate (ESL elements) (Q9 mesh [4 × 4])

Mesh		$S = 4$			$S = 50$		
		1	2	3	1	2	3
3D exact [8]		57,074.5	191,301	250,769	618.118	15,681.6	21,492.8
cf. [2]		58,216.1 (+2.00%)	196,018 (+2.46%)	268,650 (+7.13%)	618.435 (+0.05%)	15,684.0 (+0.01%)	21,499.4 (+0.03%)
ED4	SI	58,740.3 (+2.91%)	194,660 (+1.75%)	254,787 (+1.60%)	618.913 (+0.12%)	15,698.9 (+0.11%)	21,502.5 (+0.04%)
	NI	58,765.7 (+2.96%)	194,662 (+1.75%)	254,798 (+1.60%)	625.190 (+1.14%)	15,698.9 (+0.11%)	21,502.5 (+0.04%)
	CF	58,713.8 (+2.87%)	194,592 (+1.72%)	254,740 (+1.58%)	618.464 (+0.05%)	15,693.5 (+0.07%)	21,497.8 (+0.02%)
ED3	SI	58,845.6 (+3.10%)	195,842 (+2.37%)	259,649 (+3.54%)	618.999 (+0.14%)	15,699.6 (+0.11%)	21,504.8 (+0.05%)
	NI	58,870.7 (+3.14%)	195,894 (+2.40%)	259,654 (+3.54%)	625.279 (+1.23%)	15,699.3 (+0.11%)	21,504.8 (+0.05%)
	CF	58,818.6 (+3.05%)	195,825 (+2.36%)	259,586 (+3.51%)	618.550 (+0.07%)	15,694.2 (+0.07%)	21,500.1 (+0.03%)
ED2	SI	69,537.1 (+21.8%)	195,930 (+2.42%)	262,267 (+4.58%)	620.753 (+0.42%)	15,700.2 (+0.11%)	21,510.0 (+0.08%)
	NI	69,555.8 (+21.8%)	195,930 (+2.42%)	262,271 (+4.58%)	628.575 (+1.69%)	15,700.2 (+0.11%)	21,510.0 (+0.08%)
	CF	68,413.7 (+19.8%)	195,860 (+2.38%)	261,780 (+4.39%)	620.229 (+0.34%)	15,694.9 (+0.08%)	21,505.2 (+0.05%)
ED1	SI	74,232.1 (+30.0%)	195,842 (+2.37%)	266,411 (+6.23%)	690.338 (+11.68%)	15,700.3 (+0.11%)	21,512.7 (+0.09%)
	NI	74,249.8 (+30.0%)	195,930 (+2.42%)	262,271 (+4.59%)	688.575 (+11.4%)	15,700.2 (+0.12%)	21,510.0 (+0.08%)
	CF	74,105.9 (+29.8%)	196,021 (+2.47%)	266,337 (+6.21%)	689.867 (+11.6%)	15,695.0 (+0.09%)	21,498.5 (+0.03%)

SI and NI indicate respectively selected, and normal integration. CF refers to closed form solution [22].

0.596%, 0.060% and 0.020% for $S = 4$ and 0.071%, 0.053% and 0.003% for $S = 50$.

8.2. Hybrid sandwich plate

The first three circular frequencies of the simply supported hybrid sandwich plate have been listed in Tables 5–7 for different finite elements. In this case, the results are compared to the exact solution [8] and to closed-form ones [2,22]. In particular the latter one is the analytical solution that uses the same unified formulation of the present paper and it is indicated in the table with the letters CF. The mesh has been limited to $[4 \times 4]$ for computational time reasons while the element is Q9 which has shown the best

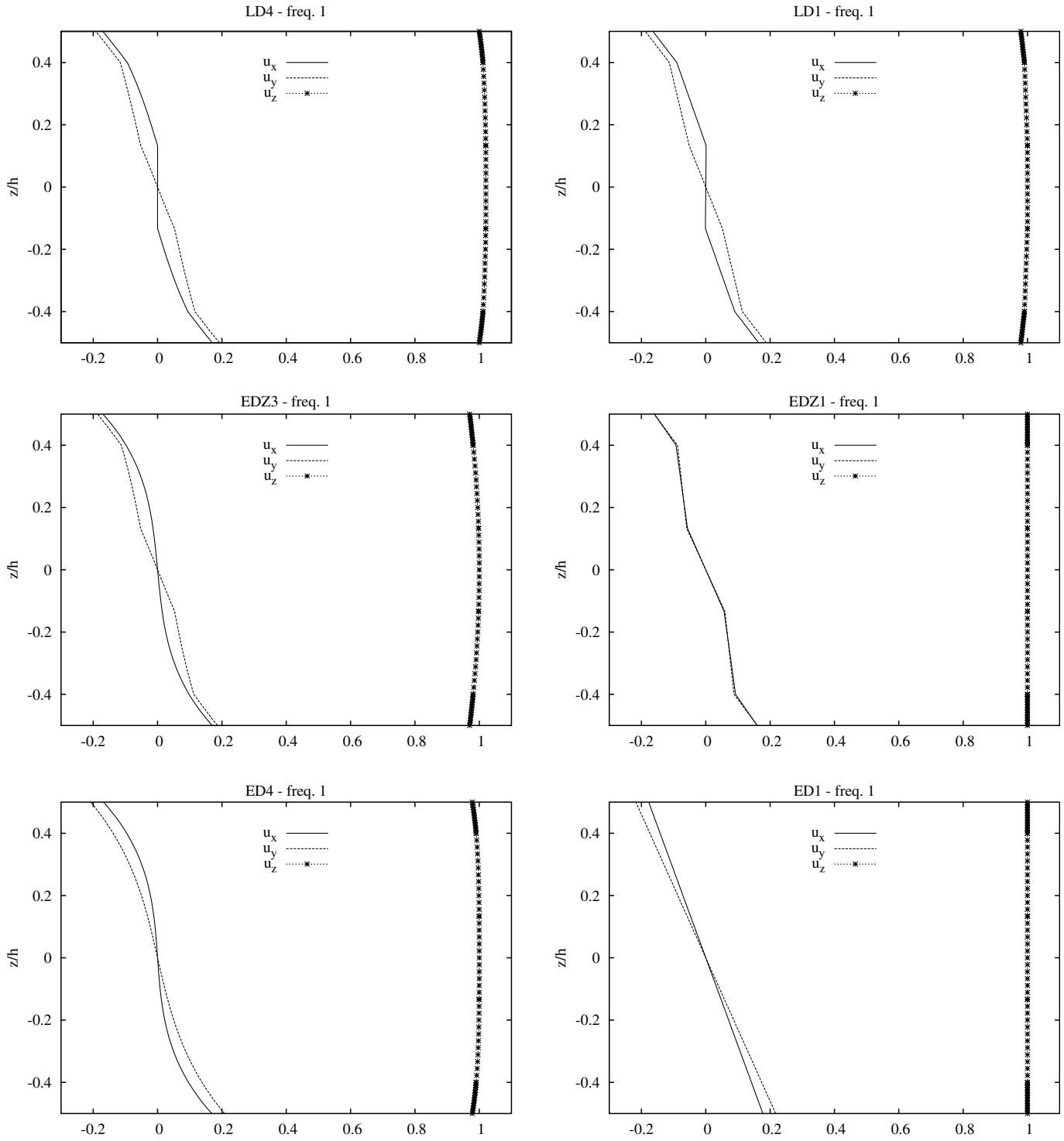

Fig. 5. Displacement through-thickness distribution for the first thickness frequency for the hybrid sandwich plate ($a/h = 4$) and different finite elements.

convergence rate. The two integration methods have been compared showing the benefits of the reduced integration in the alleviation of the shear locking mechanism.

Fig. 5 shows the through-thickness mode related to the fundamental frequency for various finite elements.

9. Conclusions

The proposed numerical solution has shown a very good agreement with the analytical one [22] based on the same unified formulation. LD3 and LD4 elements lead to results very close to the 3D exact solution [8]. In general, all the LW elements performed better than ESL ones even if higher order ESL elements (ED3, ED4) gave acceptable results. The introduction of the Murakami's function had a positive effect on the evaluation of the fundamental frequency (see Fig. 5).

For LDx ($x = 1,2,3,4$) elements, an increase of the order of the expansion has a very small effect; in contrast, EDx elements are more sensible to the order of the expansion. In particular for thick plates, at least a third order element (ED3) is required to achieve an error around 3.1% (on the fundamental frequency) with respect to the exact solution while for thin plates a quadratic expansion (ED2) can be sufficient.

Fig. 5 shows how the ED1 finite element, whose solution is very close to the one of the classical FSDT based models, is unable to catch the through-thickness variation of the displacement variables u_x and u_y.

This paper has extended the previous works by Carrera by developing new finite elements for piezolaminated plates. Since the aim of the present paper was to verify the numerical solution of the unified formulation, the presented results have been limited at the moment, to free-vibration analysis. Future developments will focus on the assessment of the performances of the present elements for the static analysis of multilayered plates embedding piezoelectric layers for both sensor and actuator applications as already done in closed-form solution in [22]. A second step forward will interest the implementation of a mixed variational principle, as done in [23], able to completely fulfill the C_z^0 requirements.

References

[1] Benjeddou A. Advances in piezoelectric finite element modeling of adaptive structural elements: a survey. Comput Struct 2000;76:347–63.

[2] Benjeddou A, Deü J-F. A two dimensional closed-form solution for the free-vibrations analysis of piezoelectric sandwich plates. Int J Solids Struct 2001;39:1463–86.

[3] Touratier M, Ossadzow-David C. Multilayered piezoelectric refined plate theory. Am Inst Aeronaut Astronaut J 2003;41(1):90–9.

[4] Carrera E. An assessment of mixed and classical theories for thermal stress analysis of orthotropic plates. J Thermal Stresses 2000;23:797–831.

[5] Carrera E. Historical review of zig-zag theories for multilayered plates and shells. Appl Mech Rev 2003;56:287–308.

[6] Tang YY, Noor AK, Xu K. Assessment of computational models for thermoelectroelastic multilayered plate. Comput Struct 1996;61(5):915–33.

[7] Saravanos DA, Heyliger PR. Mechanics and computational models for laminated piezoelectric beams, plates and shells. Appl Mech Rev 1999;52(10):302–20.

[8] Heyliger PR, Saravanos DA. Exact free vibration analysis of laminated plates with embedded piezoelectric layers. J Acoust Soc Am 1995;98(3):1547–57.

[9] Mitchell JA, Reddy JN. A refined hybrid plate theory for composite laminates with piezoelectric laminate. Int J Solids Struct 1995;32(12):2345–67.

[10] Carrera E. Theories and finite elements for multilayered anisotropic, composite plates and shells. Arch Comput Methods Eng, State art Rev 2002;9:87–140.

[11] Carrera E, Demasi L. Multilayered finite plate element based on Reissner mixed variational theorem. Part I: theory and part II: numerical analysis. Int J Numer Methods Eng 2002;55:191–231 and 253–91.

[12] Robaldo A, Benjeddou A, Carrera E. Unified formulation for piezothermoelastic analysis of multilayered plates. Research report of the Laboratory for Engineering of Mechanical Systems and Materials (LISMMA), High Institute of Mechanics at Paris (ex. ISMCM).

[13] Murakami H. Assessment of plate theories for treating the thermomechanical response of layered plates. Compos Eng 1993;3(2):137–143.

[14] Chandrashekhara K, Tenetti R. Thermally induced vibrations suppression of laminated plates with piezoelectric sensors and actuators. Smart Mater Struct 1995;4:281–90.

[15] Heyliger PR, Ramirez G, Saravanos DA. Coupled discrete-layer finite elements for laminated piezoelectric plates. Commun Numer Methods Eng 1994;10:971–81.

[16] Suleman A, Venkayya VB. A simple finite element formulation for a laminated composite plate with piezoelectric layers. J Intell Mater Syst Struct 1995;6:776–82.

[17] Saravanos DA, Heyliger PR, Hopkins DA. Layewise mechanics and finite element for the dynamic analysis of piezoelectric composite plates. Int J Solids Struct 1997;34(3):359–78.

[18] Correia VMF, Gomes MAA, Suleman A, Soares CMM, Soares CAM. Modeling and design of adaptive composite structures. Comput Methods Appl Mech Eng 2000;185:325–46.

[19] Carrera E. An improved Reissner–Mindlin type model for the electromechanical analysis of multilayered plates including piezo-layers. J Intell Mater Syst Struct 1997;8:232–48.

[20] Garcia Lage R, Mota Soares CM, Mota Soares CA, Reddy JN. Modelling of piezolaminated plates using layerwise mixed finite elements. Comput Struct 2004;82:1849–63.

[21] Ikeda T. Fundamentals of piezoelectricity. Oxford: Oxford University Press; 1996.

[22] Ballhause D. Assessment of multilayered theories for piezoelectric plates using a unified formulation. Master Thesis. Universität Stuttgart, Institut für Statik und Dynamik der Luft-und Raumfahrtkonstruktionen.

[23] Benjeddou A, Andrianarison O. A piezoelectric mixed variational theorem for smart multilayered composites. Mech Adv Mater Struct 2005;12(1):1–12.